Better performance of quantum batteries in different environments compared to closed batteries

Shu-Qian Liu,[1] Lu Wang,[1] Hao Fan,[1] Feng-Lin Wu,[1,2] and Si-Yuan Liu[1,2,*]
[1]*Institute of Modern Physics, Northwest University, Xi'an 710127, China*
[2]*Shaanxi Key Laboratory for Theoretical Physics Frontiers, Xi'an 710127, China*

(Received 5 January 2024; accepted 27 March 2024; published 11 April 2024)

We construct a central-spin battery model affected by noise or thermal bath and consider the impact of environment on battery performance. In a noisy environment, we show that the steady-state energy and ergotropy are related to the number of spins exposed to the noisy channel. In addition, we reveal the relationship between the steady-state energy and ergotropy with the quantum information lost in the battery. In a thermal bath, we find that the higher the mean occupation number of the thermal bath, the greater the steady-state energy. In particular, we find that, in two different environments, the steady-state energy and ergotropy are related to the effective magnetic-field strength of battery B, but not charger h. It is worth noting that, in the central-spin model, when B is a constant and $|h/B-1|$ reaches a certain value, the steady-state energy and ergotropy with noise or thermal bath are always greater than or equal to the maximum energy and ergotropy of the corresponding closed battery. At the same time, we generalize the conclusions to the two-qubit, two-harmonic-oscillator, and harmonic-oscillator-qubit models.

DOI: 10.1103/PhysRevA.109.042411

I. INTRODUCTION

Batteries, as a type of energy storage device, play a crucial role in human technology and social life. With the rapid development of the device miniaturization, studying the principles of energy storage and extraction in the molecular and atomic-scale systems has become an important research topic. In 2013, Alicki and Fannes first introduced the concept of quantum battery and found that the global operation can extract more work from a multiqubit system compared to local operation [1]. Since then, researchers have constructed a series of different quantum battery models using various quantum systems, such as Dicke or Rabi battery models, spin chain battery models, central-spin battery models, and so on. The performance of quantum battery, such as energy, ergotropy, and capacity, were extensively studied [2–10]. In addition, it is verified that quantum resources such as quantum entanglement and coherence play an important role in improving the performance of quantum batteries [11–15]. Moreover, quantum batteries have been implemented in experiments [16,17].

However, in the experimental implementation of quantum batteries, the system inevitably interacts with the environment. This leads to the system experiencing dissipation processes, such as decoherence and entanglement sudden death, which will affect the performance of the system negatively. Quantum batteries experience different physical processes when acting in different environments, which leads to different performance of the batteries [18–20]. In recent years, researchers have used different methods to improve the performance of quantum batteries in different environments [18,21–36]. Among them, how to utilize the physical properties of the environment itself to achieve efficient energy storage and extraction is a very significant topic in quantum battery research. The performance of a closed central-spin battery has been investigated [8,11]. This battery model has played a significant role in studying the relationship between the storage capacity of a quantum battery and the number of cells of battery and charger [8]. In addition, in a closed central-spin battery, the inverse relationship between ergotropy and entanglement at the end of the charging process has been rigorously proven [11]. In addition, the central-spin model has been implemented in experiments [37–41], which also provided great assistance for the experimental implementation of the central-spin quantum battery. Therefore, it is of great significance to study the central-spin battery that interacts with the environment.

In this paper, we study the performance of central-spin battery in two different environments, including a noisy environment and a thermal bath. In the phase-flip noisy environment, we consider the effects of number of spins exposed to the noisy channel and the strength of noise on the battery performance, respectively. We also connect the changes of battery performance with the quantum information lost in the battery during the evolution process. In the thermal bath, we analyze the effects of the global or local operations and the mean occupation number of the thermal bath on the battery performance. Specifically, in the above environments, by adjusting the effective external magnetic-field strength of the battery and charger, we find that the steady-state energy and ergotropy are always greater than or equal to the maximum energy and ergotropy of the corresponding closed system. We generalize these results to other battery models, both analytically and numerically.

This paper is organized as follows. In Sec. II, we introduce the central-spin battery, master equation method, and the definitions of quantum battery energy and ergotropy. In

*lsy5227@163.com

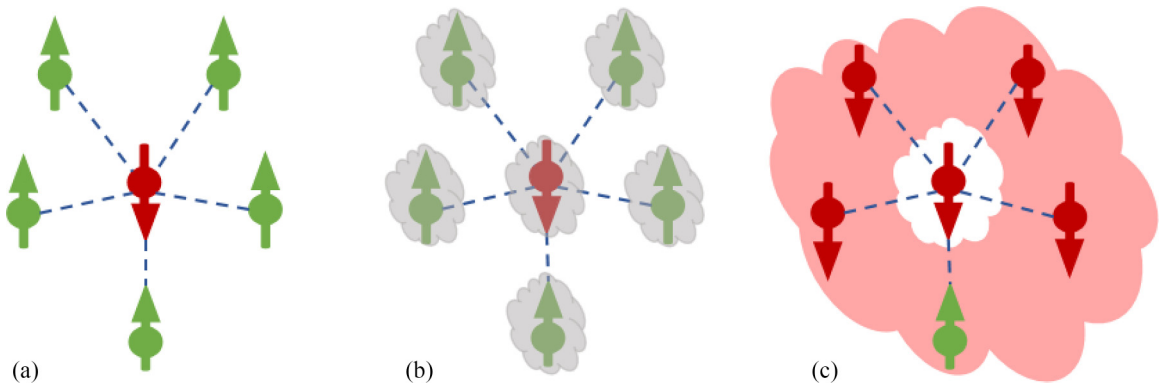

FIG. 1. Panel (a) is a schematic illustration of the closed central-spin model, showing the process of energy transfer from the charger in the excited state to the battery in the ground state through interaction. Panel (b) is a schematic illustration of the central-spin model in a noisy environment, showing the process in which the charger in the excited state transfers energy to the battery in the ground state through interaction, and both the battery and charger are affected by noise. Panel (c) shows the schematic illustration of the central-spin model in a thermal bath, showing that the thermal bath interacts with the charger and then transfers energy to the battery through the charger. Here, the green (red) arrow represents spin up (down), the blue dashed line represents the interaction between the battery and charger, the gray shadow represents noise, and the pink shadow represents a thermal bath.

Sec. III, we discuss the performance of the central-spin battery in the phase-flip noisy environment. In Sec. IV, we analyze the performance of the central-spin battery in a thermal bath. In Sec. V, we draw the conclusion for our work.

II. MODEL OF CENTRAL-SPIN BATTERY AND PERFORMANCE PARAMETERS

A. Model of central-spin battery

The central spin model is a system consisting of N_b central spins surrounded by N_c spins, as shown in Fig. 1. The Hamiltonian can be written as

$$H = H_B + H_C + H_I, \tag{1}$$

$$H_B = BS^z, \tag{2}$$

$$H_C = hJ^z, \tag{3}$$

$$H_I = A(S^+J^- + S^-J^+) + 2\Delta S^z J^z. \tag{4}$$

In the above expression, $S^\alpha = \sum_{i=1}^{N_b} \sigma_i^\alpha/2$ represents the total spin operator for N_b battery spins, $J^\alpha = \sum_{j=1}^{N_c} \sigma_j^\alpha/2$ represents the total spin operator for N_c charger spins, $\sigma_{i(j)}^\alpha (\alpha = x, y, z)$ is the Pauli operator. $S^\pm = S^x \pm iS^y$ and $J^\pm = J^x \pm iJ^y$ are spin ladder operators for the battery and charger, respectively. B and h represent the effective external magnetic-field strength of battery and charger. A and Δ are the spin flip-flop interaction strength and Ising interaction strength.

At initial time, the battery is in the ground state, which can be expressed as $|0\rangle_b \equiv |\downarrow_1, \downarrow_2, \downarrow_3, \ldots, \downarrow_{N_b}\rangle$. The charger is represented by the Dicke state, i.e., $|m\rangle_c \equiv \frac{1}{\sqrt{\binom{N_c}{m}}} \sum_k P_k(|\uparrow_1, \uparrow_2, \uparrow_3, \ldots, \uparrow_m, \downarrow_{m+1}, \ldots, \downarrow_{N_c}\rangle)$, where m represents the number of up spins of all charger spins, $\frac{1}{\sqrt{\binom{N_c}{m}}} = \frac{1}{\sqrt{N_c!/[m!(N_c-m)!]}}$ indicates the probability that the charger is in a certain state, and P_k indicates all possible arrangements of charger spins. It is worth noting that when $m \ll N_c$, the central-spin model can be mapped to the Tavis-Cummings model using the Holstein-Primarkoff transform [11], the above situation is not considered in our paper.

As the battery interacts with environment, the dynamic evolution of the quantum battery can be described by the Lindblad master equation

$$\dot{\rho}(t) = -i[H, \rho(t)] + \mathcal{L}[\rho], \tag{5}$$

where $\rho(t)$ is the density matrix of the total quantum battery system at time t. The first term on the right side of Eq. (5) represents the von Neumann equation term, and the second term represents that the system experience transition, dissipation, and so on, where $\mathcal{L}[\rho] = \mathcal{L}\rho(t)\mathcal{L}^\dagger - \frac{1}{2}\{\mathcal{L}\mathcal{L}^\dagger, \rho(t)\}$ is the Lindblad superoperator.

B. Stored energy and ergotropy

Next we choose two parameters, which are the key indicators for quantifying quantum battery performance. The first one is stored energy. The energy of the battery at time t is expressed as

$$E_B(t) = \mathrm{Tr}[H_B\rho_B(t)], \tag{6}$$

where $\rho_B(t) = \mathrm{Tr}_c[|\psi(t)\rangle\langle\psi(t)|]$ is the reduced density matrix of the battery and $|\psi(t)\rangle$ describes the state of the whole system. $\Delta E_B(t) = E_B(t) - E_B(0)$ represents the energy stored in the evolution of the system at time t. The second parameter is ergotropy, which means the maximum energy that can be extracted at time t, and its expression can be written as

$$\varepsilon_B(t) = E_B(t) - \min_U \mathrm{Tr}[H_B U \rho_B(t) U^\dagger], \tag{7}$$

where U represents the unitary operator of the battery. The $\min_U \mathrm{Tr}[H_B U \rho_B(t) U^\dagger]$ is the minimum energy obtained by the unitary evolution of the battery at time t [1]. It can be obtained by rearranging the eigenvalues of the density matrix ρ_B in descending order and the eigenvalues of the Hamiltonian H_B in ascending order, i.e., $\rho_B(t) = \sum_{j\geqslant 1} r_j |r_j\rangle\langle r_j|$, $H_B = \sum_{j\geqslant 1} \varepsilon_j |\varepsilon_j\rangle\langle\varepsilon_j|$, where $r_1 \geqslant r_2 \geqslant \cdots \geqslant r_j$, $\varepsilon_1 \leqslant \varepsilon_2 \leqslant$

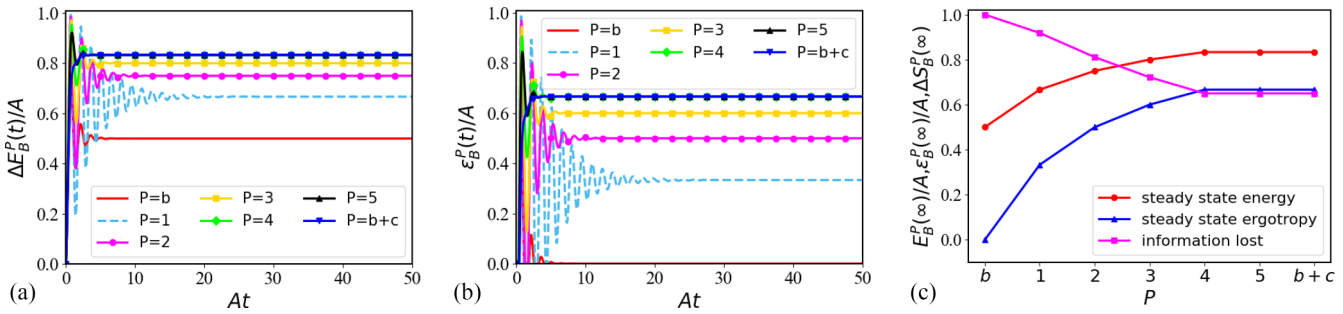

FIG. 2. Panels (a) and (b) show the changes of the stored energy $\Delta E_B^P(t)$ and ergotropy $\varepsilon_B^P(t)$ over time t. The two figures show that different numbers of spins are exposed to phase-flip noise. Here $P = b$ (red solid line) indicates that the battery is exposed to phase-flip noise, $P = b + c$ (dark blue downward triangles) indicates that the battery and charger are exposed to the phase-flip noise, $P = 1, 2, 3, 4, 5$ (from light blue dashed line to black upward triangles) indicates the number of spins in the charger exposed to phase-flip noise. Panel (c) shows the steady-state energy $E_B^P(\infty)$ (red dots), ergotropy $\varepsilon_B^P(\infty)$ (dark blue triangles), and the quantum information lost in the battery $\Delta S_B^P(\infty)$ (purple squares) as a function of the number of spins exposed to the phase-flip noise P. The parameters $N_c = 5$, $m = 5$, $N_b = 1$, $B = 1$, $h = 1$, $A = 1$, $\Delta = 0$, $\kappa = 1$.

$\cdots \leqslant \varepsilon_j$. Equation (7) can be rewritten as [9]

$$\varepsilon_B(t) = E_B(t) - \sum_j r_j \varepsilon_j. \tag{8}$$

If the system is closed, energy will only flow between the battery and charger. Therefore, the maximum energy that can be stored is generally selected as the stored energy, expressed as $E_{\max} = \max[\Delta E_B(t)]$, the maximum energy that can be extracted is called the maximum ergotropy $\varepsilon_{\max} = \max[\varepsilon_B(t)]$. Compared with the closed system, the energy and ergotropy of the battery in the open system have no periodicity, but oscillate in the initial stage and reach a steady state after a period of time. When reaching the steady state, the energy that can be stored is called the steady-state energy $E_B(\infty)$, and the maximum energy that can be extracted is called the steady-state ergotropy $\varepsilon_B(\infty)$ [27]. The larger the $E_B(\infty)$ and $\varepsilon_B(\infty)$, the more energy the battery can be stored and extracted at steady state.

III. PERFORMANCE OF THE CENTRAL-SPIN BATTERY IN A NOISY ENVIRONMENT

Consider the charger contains five spins ($N_c = 5$) and the battery contains one spin ($N_b = 1$), the noisy type is phase-flip noise, and Eq. (5) can be specifically written as

$$\begin{aligned}\dot{\rho}(t) = & -i[H, \rho(t)] + \kappa(\sigma_z \otimes I^{\otimes 5})[\rho] \\ & + \kappa(I \otimes \sigma_z \otimes I^{\otimes 4})[\rho] + \cdots \\ & + \kappa(I \otimes I^{\otimes 4} \otimes \sigma_z)[\rho],\end{aligned} \tag{9}$$

where κ represents the strength of phase-flip noise. The first term represents the von Neumann equation term on the right side of Eq. (9). The second term indicates that the battery spin is exposed to the phase-flip noise. From the third to the last terms indicate that one of the charger spins is exposed to the phase-flip noise.

A. Number of spins exposed to the phase-flip noise and the strength of noise

Set the initial state of the system to $|\psi_0\rangle = |0\rangle_b \otimes |m\rangle_c$ ($m = 5$), where $|m\rangle_c$ is the Dicke state. Let's consider the effect of number of spins exposed to the phase-flip noise P on the stored energy $\Delta E_B^P(t)$ and ergotropy $\varepsilon_B^P(t)$ of the battery, as shown in Figs. 2(a) and 2(b). We observe that when the battery is exposed to phase-flip noise, the steady-state energy is $E_B^b(\infty) = 0.5$, the steady-state ergotropy is $\varepsilon_B^b(\infty) = 0$. Moreover, the steady-state energy and ergotropy increase with the increasing number of spins exposed to phase-flip noise in the charger. When the battery and charger are completely exposed to phase-flip noise, the steady-state energy is $E_B^{b+c}(\infty) \approx 0.833$, the steady-state ergotropy is $\varepsilon_B^{b+c}(\infty) \approx 0.667$. Because phase-flip noise can cause quantum information loss in the system, we use von Neumann entropy to measure the quantum information of the density matrix ρ [42]:

$$S(\rho) = -\mathrm{Tr}(\rho \log_2 \rho). \tag{10}$$

So the quantum information lost in the battery during the evolution process can be written as

$$\Delta S_B(t) = S[\rho_B(t)] - S[\rho_B(0)]. \tag{11}$$

We study the relationship between the $\Delta S_B^P(t)$ and the number of spins exposed to the phase-flip noise P, as shown in Fig. 2(c). When $P = b$, we find that the $\Delta S_B^b(\infty) = 1$, the quantum information is completely lost, and the battery is in a completely mixed state, so the energy cannot be extracted. However, when $P = 1$, 2, 3, 4, 5 and $b + c$, the quantum information of the battery will not be completely lost, the steady state is not completely mixed, and the energy can be partially extracted. The $E_B^P(\infty)$ and $\varepsilon_B^P(\infty)$ are correlated with the $\Delta S_B^P(\infty)$ negatively, as shown in Fig. 2(c). When the battery and charger are exposed to the phase-flip noise, the battery has the best performance. So in the following study, we consider the case that the battery and charger are exposed to phase-flip noise.

In addition, we find that when the battery and charger are completely exposed to phase-flip noise, the value of steady-state energy can be written as 5/6. This seems unusual. We

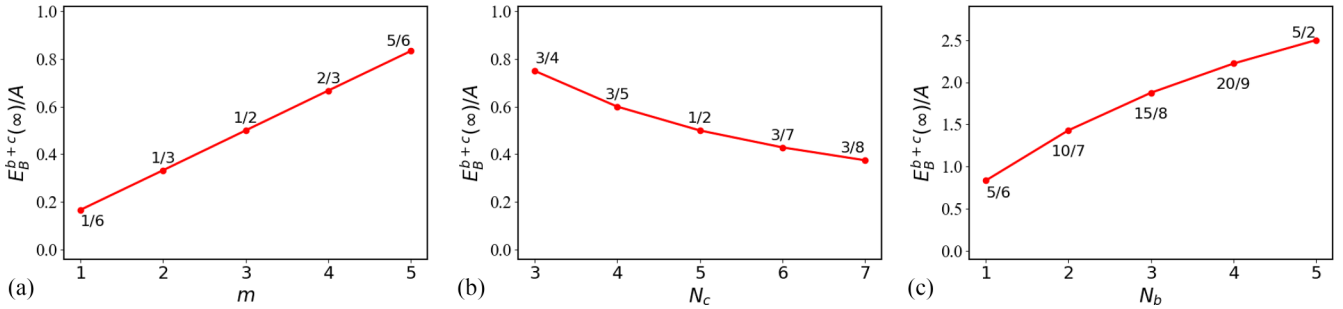

FIG. 3. Panel (a) shows the variation of steady-state energy $E_B^{b+c}(\infty)$ with the number of up spins of all charger spins m, here $N_b = 1$, $N_c = 5$. Panel (b) shows the variation of steady-state energy $E_B^{b+c}(\infty)$ with the spin numbers in charger N_c, here $N_b = 1, m = 3$. Panel (c) shows the variation of steady-state energy $E_B^{b+c}(\infty)$ with the spin numbers in battery N_b, here $N_c = 5, m = 5$. The other parameters are same as Fig. 2.

summarize the law by numerical calculations, as shown in Fig. 3. It was found that when the battery is in the ground state, the steady-state energy is

$$E_B^{b+c}(\infty) = N_b \frac{m}{N_b + N_c}, \tag{12}$$

where m represents the number of up spins of all charger spins. N_b and N_c are the spin numbers in battery and charger, respectively. Phase-flip noise describes the loss of quantum information in a system without the loss of energy [42]. So, when the phase-flip noise is applied to each charger spin in the excited state, it does not reduce the energy of each charger spin. When the phase-flip noise is applied to each battery spin in the ground state, it does not increase the energy of each battery spin. As an environment, phase-flip noise will stabilize the whole system. Because the steady-state density matrix of all the spins is the same, the energy can only be distributed averagely throughout the system to achieve stability. So the steady-state energy can be expressed as Eq. (12). Since the steady-state energy of the battery is determined, the steady-state density matrix is determined. According to Eq. (8), the steady-state ergotropy can be determined.

The strength of noise κ is also an important parameter affecting the performance of central-spin quantum battery in an open environment. We discuss the influence of the strength of noise κ on the stored energy $\Delta E_B^{b+c}(t)$ and ergotropy $\varepsilon_B^{b+c}(t)$, as shown in Figs. 4(a) and 4(b). We find that the change of κ does not affect the $E_B^{b+c}(\infty)$ and $\varepsilon_B^{b+c}(\infty)$. Before reaching the steady state, the oscillation amplitude of the stored energy and ergotropy of the battery, and the time to reach the steady state are related to the κ. The smaller the κ, the greater the oscillation amplitude of the stored energy and ergotropy of the battery, and the longer the time to reach the steady state. At the same time, we study the change of ΔS_B^{b+c} with κ. From Fig. 4(c), we find that the ΔS_B^{b+c} does not change with κ. Because the ΔS_B^{b+c} is unchanged, which leads to an unchanged mixed degree of the steady state, the $E_B^{b+c}(\infty)$ and $\varepsilon_B^{b+c}(\infty)$ remain unchanged.

B. Effective magnetic-field strength of battery and charger

We investigate the changes of the steady-state energy $E_B^{b+c}(\infty)$ and ergotropy $\varepsilon_B^{b+c}(\infty)$ of the battery with the effective magnetic-field strength of battery B and charger h, respectively, as shown in Fig. 5. Through Fig. 5(a), we find that the $E_B^{b+c}(\infty)$ and $\varepsilon_B^{b+c}(\infty)$ increase proportionally with the increase of B. This is because the change of B does not affect the steady-state density matrix of the battery, but the energy eigenvalue is proportional to B. On the contrary, Fig. 5(b) shows that the $E_B^{b+c}(\infty)$ and $\varepsilon_B^{b+c}(\infty)$ are independent of h. This is because h neither changes the steady-state density matrix nor the energy eigenvalue of the battery.

In a closed central-spin system, when $B = h$, that is, resonance, the maximum energy $E_{\max}$ and ergotropy $\varepsilon_{\max}$ reach the peak value [8]. According to the results in the above paragraph, when the system is in the phase-flip noisy environment, the $E_B^{b+c}(\infty)$ and $\varepsilon_B^{b+c}(\infty)$ are only related to B and not related to h. In other words, when B is a constant, the

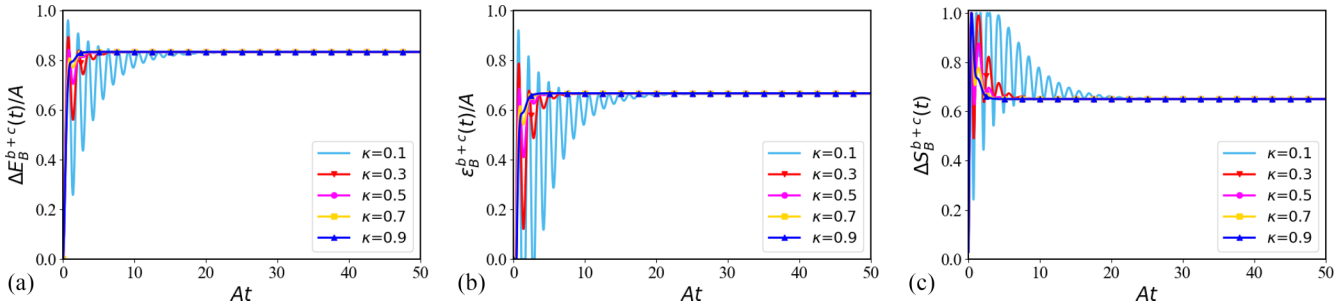

FIG. 4. Panels (a) and (b) show the evolutions of the stored energy $\Delta E_B^{b+c}(t)$ and ergotropy $\varepsilon_B^{b+c}(t)$ over time t with the different strength of noise $\kappa = 0.1, 0.3, 0.5, 0.7, 0.9$, respectively (from light blue solid line to dark blue upward triangles). Panel (c) shows the evolution of quantum information lost $\Delta S_B^{b+c}(t)$ over time t in the battery with the different strength of noise $\kappa = 0.1, 0.3, 0.5, 0.7, 0.9$, respectively (from light blue solid line to dark blue upward triangles). The other parameters are same as Fig. 2.

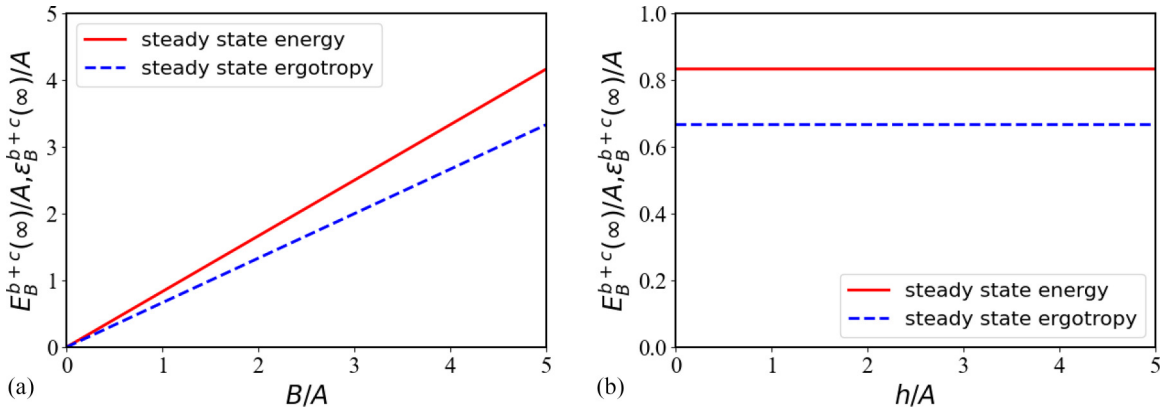

FIG. 5. Panel (a) shows the variations of the steady-state energy $E_B^{b+c}(\infty)$ (red solid line) and ergotropy $\varepsilon_B^{b+c}(\infty)$ (dark blue dashed line) with the effective magnetic-field strength of battery B. Panel (b) shows the variations of the steady-state energy $E_B^{b+c}(\infty)$ (red solid line) and ergotropy $\varepsilon_B^{b+c}(\infty)$ (dark blue dashed line) with the effective magnetic-field strength of charger h. The other parameters are same as Fig. 2.

value of h/B only affects the $E_{\max}$ and $\varepsilon_{\max}$ in the closed central-spin system, and does not affect the $E_B^{b+c}(\infty)$ and $\varepsilon_B^{b+c}(\infty)$ in the phase-flip noisy environment. We calculate the $E_{\max}$ and $\varepsilon_{\max}$ in the closed central-spin system and the $E_B^{b+c}(\infty)$ and $\varepsilon_B^{b+c}(\infty)$ in the phase-flip noisy environment with the change of h/B, as shown in Fig. 6. It is shown that for a closed system, when B is a constant and $|h/B-1|=0$, the $E_{\max}$ and $\varepsilon_{\max}$ can reach the peak value, and the larger the value of $|h/B-1|$, the smaller the $E_{\max}$ and $\varepsilon_{\max}$. While the $E_B^{b+c}(\infty)$ and $\varepsilon_B^{b+c}(\infty)$ in the phase-flip noisy environment are independent of $|h/B-1|$. So, we conclude that in the central-spin system, when B is a constant and $|h/B-1|$ reaches a certain value, the $E_B^{b+c}(\infty)$ and $\varepsilon_B^{b+c}(\infty)$ in the phase-flip noisy environment will always be greater than or equal to the $E_{\max}$ and $\varepsilon_{\max}$ in the corresponding closed system.

In addition, we also proved this conclusion in other battery models [23]. We consider the steady-state energy $E_B^{b+c}(\infty)$ and ergotropy $\varepsilon_B^{b+c}(\infty)$ under the phase-flip noise of the two-qubit, two-harmonic-oscillator, and harmonic-oscillator-qubit models, and compare them with the maximum energy $E_{\max}$ and ergotropy $\varepsilon_{\max}$ of the corresponding closed system.

Considering that the charger C and battery B are qubits, the total Hamiltonian can be written as

$$H_1 = \omega_b \frac{\sigma_B^z}{2} + \omega_c \frac{\sigma_C^z}{2} + g(\sigma_C^- \sigma_B^+ + \sigma_C^+ \sigma_B^-), \tag{13}$$

where ω_c is the energy level spacing of the charger, ω_b is the energy level spacing of the battery, and g is the coupling strength of the battery and charger. $\sigma_{B,C}^{x,y,z}$ represent the Pauli operators acting on system B or C, and $\sigma_{B,C}^{\pm} = (\sigma_{B,C}^x \pm i\sigma_{B,C}^y)/2$ represent the up and down operators of the qubit.

Assume that the battery is in the ground state and the charger is in the excited state at the initial time, and consider that the charger and battery are exposed to phase-flip noise. We calculate the $E_{\max}$ and $\varepsilon_{\max}$ in the closed system and the $E_B^{b+c}(\infty)$ and $\varepsilon_B^{b+c}(\infty)$ in the phase-flip noisy environment with the change of ω_c/ω_b, as shown in Fig. 7. We can find that the steady-state energy is $E_B^{b+c}(\infty)=0.5$, steady-state ergotropy is $\varepsilon_B^{b+c}(\infty)=0$. The conclusion is verified that when ω_b is a constant and $|\omega_c/\omega_b-1|$ reaches a certain value, the $E_B^{b+c}(\infty)$ and $\varepsilon_B^{b+c}(\infty)$ in the phase-flip noisy environment will always be greater than or equal to the $E_{\max}$ and $\varepsilon_{\max}$ of the corresponding closed system. Similarly, we

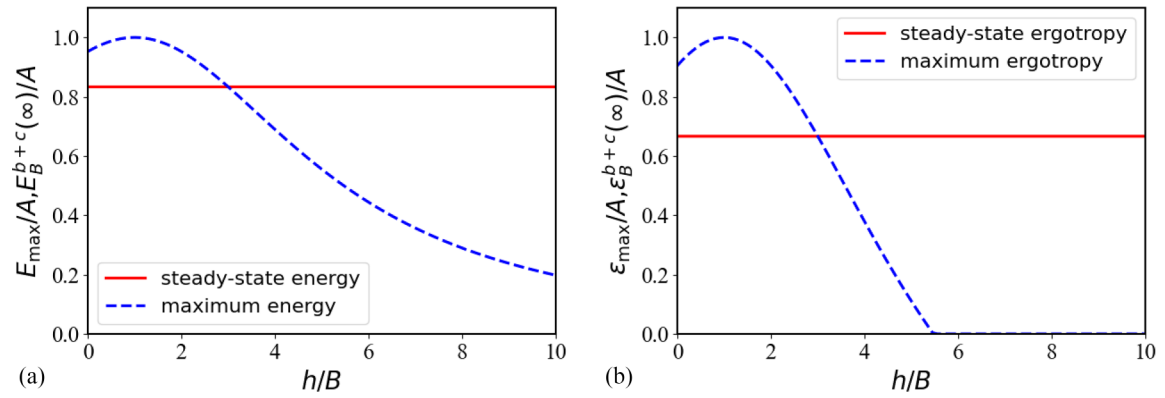

FIG. 6. Panel (a) shows the variations of maximum energy $E_{\max}$ (dark blue dashed line) in the closed central-spin system and steady-state energy $E_B^{b+c}(\infty)$ (red solid line) in the phase-flip noisy environment with h/B. Panel (b) shows the variations of maximum ergotropy $\varepsilon_{\max}$ (dark blue dashed line) in the closed central-spin system and steady-state ergotropy $\varepsilon_B^{b+c}(\infty)$ (red solid line) in the phase-flip noisy environment with h/B. Here $N_c=5, m=5, N_b=1, B=1, A=1, \Delta=0, \kappa=1$.

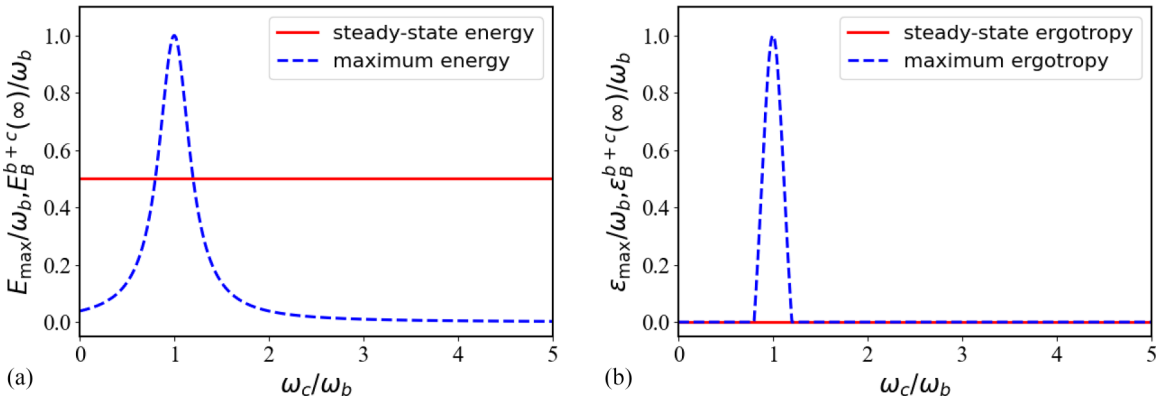

FIG. 7. Panel (a) shows that the maximum energy $E_{\max}$ (dark blue dashed line) in the closed two-qubit system and steady-state energy $E_B^{b+c}(\infty)$ (red solid line) in the phase-flip noisy environment vary with ω_c/ω_b changes. Panel (b) shows that the maximum ergotropy $\varepsilon_{\max}$ (dark blue dashed line) in the closed two-qubit system and steady-state ergotropy $\varepsilon_B^{b+c}(\infty)$ (red solid line) in the phase-flip noisy environment vary with ω_c/ω_b changes. Here $\omega_b = 1$, $g = 0.1$, $\kappa = 1$.

can get this conclusion in the two-harmonic-oscillator and harmonic-oscillator-qubit models, see Appendix A. When the environment is bit-flip noise, we find that there are similar conclusions in the above four models, see Appendix B. In three models, we analytically demonstrate the variation of $E_{\max}$ and $\varepsilon_{\max}$ with ω_c, see Appendix C.

IV. PERFORMANCE OF THE CENTRAL-SPIN BATTERY IN A THERMAL BATH

Because it is difficult to reach absolute zero under actual experimental conditions, quantum systems are often in a thermal bath. It is necessary to study the performance of quantum battery in the thermal bath [18,24,43–47]. In this section, we mainly study the performance of the central-spin battery in a thermal bath. The charger contains five spins ($N_c = 5$) and the battery contains one spin ($N_b = 1$). At the initial moment, the system is in the state $|\psi_0\rangle = |0\rangle_b \otimes |m\rangle_c$ ($m = 1$). And consider the process where the thermal bath acts on the charger and then transfers energy to the battery through the interaction of the battery and charger.

A. Global or local operations and the mean occupation number of the thermal bath

We first consider the effect of the global or local operations of the thermal bath on the stored energy and ergotropy. Global operation refers to the thermal bath acting on all charger spins, while local operation refers to the thermal baths acting on each charger spin. The master equation for the thermal bath acting on the charger through the global operation can be written as

$$\begin{aligned}\dot{\rho}(t) =& -i[H, \rho(t)] + \gamma n_B (I \otimes J^+)[\rho] \\ &+ \gamma (n_B + 1)(I \otimes J^-)[\rho],\end{aligned} \tag{14}$$

where γ is the spontaneous emission rate of the charger, $n_B = 1/\{\exp[\omega_c/(k_B T)] - 1\}$ denotes the mean occupation number of the thermal bath. The second and third terms on the right side of Eq. (14) represent the process of the charger absorbing and releasing photons when a thermal bath acts on the five charger spins. The master equation for the thermal baths acting on the charger through the local operation can be written as

$$\begin{aligned}\dot{\rho}(t) =& -i[H, \rho(t)] + \gamma n_B (I \otimes \sigma^+ \otimes I^{\otimes 4})[\rho] \\ &+ \gamma (n_B + 1)(I \otimes \sigma^- \otimes I^{\otimes 4})[\rho] + \cdots \\ &+ \gamma n_B (I \otimes I^{\otimes 4} \otimes \sigma^+)[\rho] \\ &+ \gamma (n_B + 1)(I \otimes I^{\otimes 4} \otimes \sigma^-)[\rho].\end{aligned} \tag{15}$$

The second to the last terms on the right side of Eq. (15) represent the process of the charger absorbing and releasing photons when five thermal baths act on five charger spins, respectively. For the global or local operations of the thermal bath, we solve the stored energy $\Delta E_B(t)$ over time, as shown in Fig. 8. From the numerical results, it can be seen that regardless of whether the thermal bath acts globally or locally on the charger, the steady-state energy is the same. In addition, the steady state is a thermal state. In this state, the energy is equal to the minimum energy that can be obtained after the unitary transformation. So the steady-state ergotropy is zero [23,27]. Although the steady-state ergotropy of the battery is zero, we believe that the study of steady-state energy is of

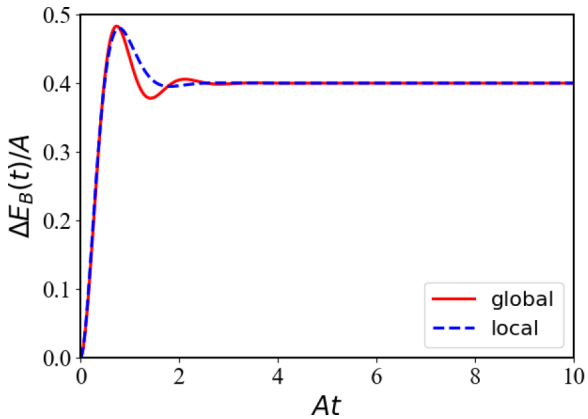

FIG. 8. The evolution of stored energy $\Delta E_B(t)$ with time t, where the red solid line represents the global operation of thermal bath on the charger, and the dark blue dashed line represents the local operation of thermal bath on the charger. The parameters $N_c = 5$, $m = 1$, $N_b = 1$, $B = 1$, $h = 1$, $A = 1$, $\Delta = 0$, $\gamma = 1$, $n_B = 2$.

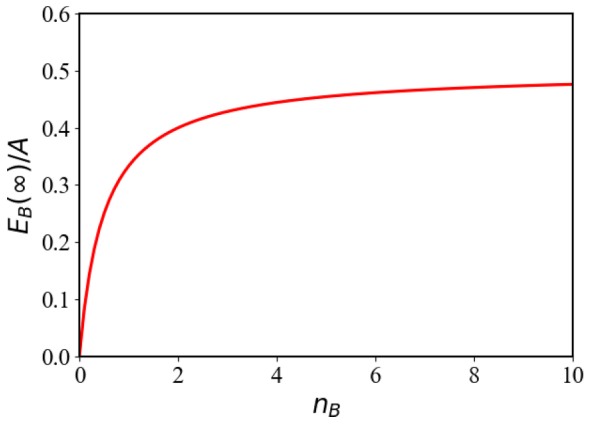

FIG. 9. The variation of steady-state energy $E_B(\infty)$ with the mean occupation number of thermal bath n_B. The other parameters are same as Fig. 8.

great significance. Ergotropy is the maximum energy that can be extracted by any unitary operations. Considering nonunitary operations, more energy will be extracted. Therefore, even if the steady-state ergotropy is zero in the current definition, it is still worthwhile to study the steady-state energy in this case.

Based on the above analysis, the influence of mean occupation number of the thermal bath n_B on the performance of central-spin battery should not be underestimated. Consider that the thermal bath acts on the charger in global operation. From Fig. 9, we can see that the $E_B(\infty)$ gradually increases with the increasing n_B and tends to a stable value.

B. Effective magnetic-field strength of battery and charger

Since the steady-state ergotropy of the battery is zero, we only calculate the steady-state energy $E_B(\infty)$ in the thermal bath with respect to the effective magnetic field of battery B and charger h, respectively, as shown in Fig. 10. Similarly, by Fig. 10(a), we find that the $E_B(\infty)$ increases proportionally with the increase of B. This is because the steady state of the battery is the thermal state, which is independent of B, and the energy eigenvalue is proportional to B. On the contrary, Fig. 10(b) shows that the $E_B(\infty)$ is independent of h. This is because the steady state and energy eigenvalues of the battery are independent of h.

In addition, we calculate the maximum energy $E_{\max}$ and ergotropy $\varepsilon_{\max}$ in the closed central-spin system and the steady-state energy $E_B(\infty)$ and ergotropy $\varepsilon_B(\infty)$ in the thermal bath with the change of h/B, as shown in Fig. 11. For a closed system, it is shown that when B is a constant and $|h/B-1|=0$, the $E_{\max}$ and $\varepsilon_{\max}$ have peak values. The $E_{\max}$ and $\varepsilon_{\max}$ decrease with the increasing $|h/B-1|$. In contrast, in the thermal bath, the value of $E_B(\infty)$ and $\varepsilon_B(\infty)$ are independent of $|h/B-1|$. Therefore, we conclude that in a central-spin system, when B is a constant and $|h/B-1|$ reaches a certain value, the $E_B(\infty)$ and $\varepsilon_B(\infty)$ in the thermal bath will always be greater than or equal to the $E_{\max}$ and $\varepsilon_{\max}$ in the corresponding closed system.

Furthermore, we consider the steady-state energy $E_B(\infty)$ and ergotropy $\varepsilon_B(\infty)$ of the battery in the thermal bath for the two-qubit, two-harmonic-oscillator, and harmonic-oscillator-qubit models, and compare them with the maximum energy $E_{\max}$ and ergotropy $\varepsilon_{\max}$ of the corresponding closed system. Let the battery in the ground state and charger in the excited state at the initial moment, the thermal bath acts on the charger. We calculate the $E_{\max}$ and $\varepsilon_{\max}$ in the closed two-qubit system and the $E_B(\infty)$ and $\varepsilon_B(\infty)$ in the thermal bath with the change of ω_c/ω_b, as shown in Fig. 12. We find that the two-qubit model is also consistent with the conclusion that when ω_b is a constant and $|\omega_c/\omega_b-1|$ reaches a certain value, the $E_B(\infty)$ and $\varepsilon_B(\infty)$ in the thermal bath will always be greater than or equal to the $E_{\max}$ and $\varepsilon_{\max}$ of the corresponding closed system. Similarly, we can get this conclusion in the two-harmonic-oscillator and harmonic-oscillator-qubit models, see Appendix A.

V. CONCLUSION

Generally speaking, the interaction between the system and environment will lead to decoherence of the system and negative effect in battery performance. Therefore, it is significant to design batteries that use the environment itself to improve performance. We considered the performance of the central-spin battery in two different environments. In the phase-flip noisy environment, we found that the steady-state

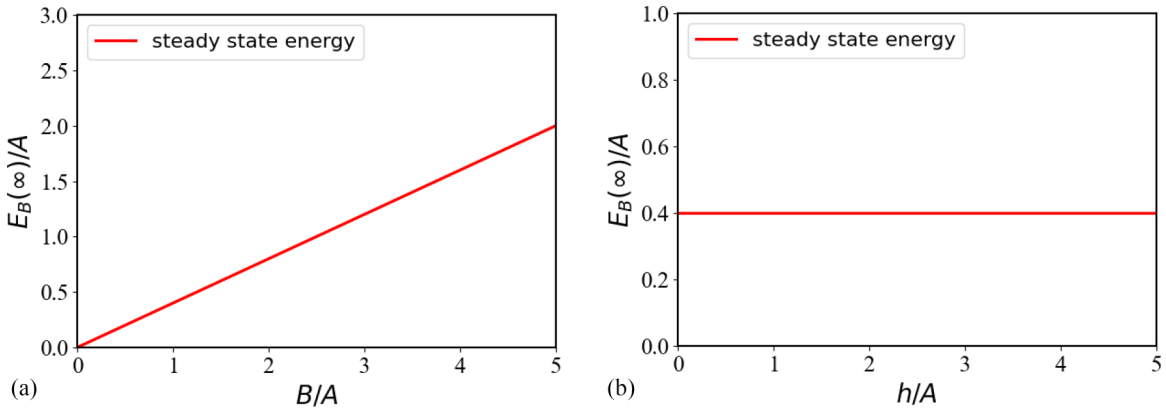

FIG. 10. Panel (a) shows the variation of steady-state energy $E_B(\infty)$ with the effective magnetic-field strength of battery B. Panel (b) shows the variation of steady-state energy $E_B(\infty)$ with the effective magnetic-field strength of charger h. The other parameters are same as Fig. 8.

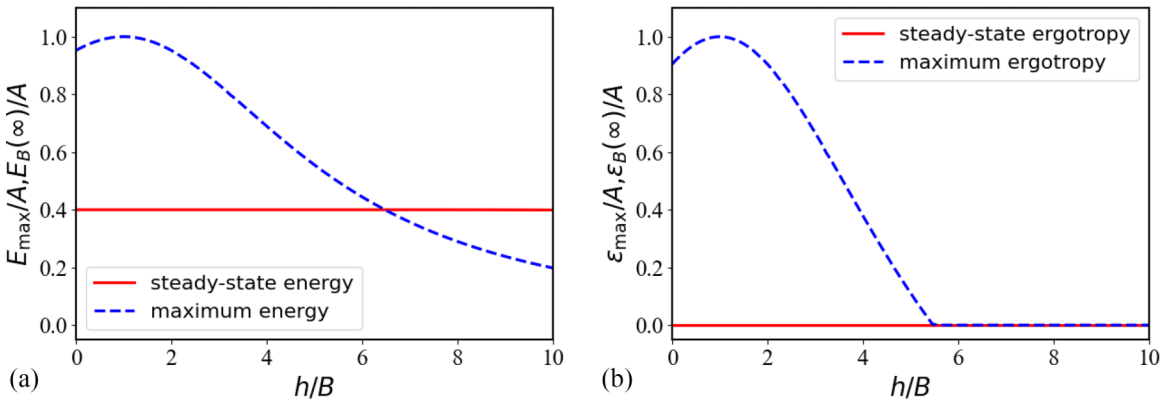

FIG. 11. Panel (a) represents the maximum energy $E_{\max}$ (dark blue dashed line) in the closed central-spin system and steady-state energy $E_B(\infty)$ (red solid line) in the thermal bath as a function of h/B. Panel (b) represents the maximum ergotropy $\varepsilon_{\max}$ (dark blue dashed line) in the closed central-spin system and steady-state ergotropy $\varepsilon_B(\infty)$ (red solid line) in the thermal bath as a function of h/B. Here $N_c = 5, m = 1$, $N_b = 1, B = 1, A = 1, \Delta = 0, \gamma = 1, n_B = 2$.

energy and ergotropy are related to the number of spins exposed to the noisy channel, but independent of the strength of noise. We investigated the relationship between the stored energy, ergotropy, and the quantum information lost in the battery during the evolution process. In addition, we found that the more information lost, the smaller the steady-state energy and ergotropy. In the thermal bath, we found that the steady-state energy and ergotropy increase with the mean occupation number of the thermal bath, independent of the global or local operations of the thermal bath.

In particular, in both of these environments, we found that the steady-state energy and ergotropy are related to the effective magnetic-field strength of battery B, but not charger h. However, the maximum energy and ergotropy of the closed central-spin system are related to B and h. When B is a constant and $|h/B - 1| = 0$, the maximum energy and ergotropy reach the peak value. The maximum energy and ergotropy decrease with the $|h/B - 1|$ increases. Therefore, it is shown that in the central-spin model, when B is a constant and $|h/B - 1|$ reaches a certain value, the steady-state energy and ergotropy in the open system (including the thermal bath, phase-flip noise, and bit-flip noise) are always greater than or equal to the maximum energy and ergotropy in the closed system. The conclusion has also been validated analytically and numerically in the two-qubit, two-harmonic-oscillator, and harmonic-oscillator-qubit models.

We believe that the results in this paper can contribute to the study of the performance of quantum batteries in open systems and our work is of great help to the experimental realization of the quantum battery.

ACKNOWLEDGMENTS

We gratefully thank Zhen-Yu Peng for the helpful discussions. This work was supported by the National Natural Science Foundation of China (Grant No. 12175179), the Peng Huanwu Center for Fundamental Theory (Grant No. 12247103), and the Natural Science Basic Research Program of Shaanxi Province (Grants No. 2021JCW-19 and No. 2019JQ-863).

APPENDIX A

Considering that the charger and battery are harmonic oscillators, the total Hamiltonian can be written as

$$H_2 = \omega_b b^\dagger b + \omega_c c^\dagger c + g(c^\dagger b + c b^\dagger), \tag{A1}$$

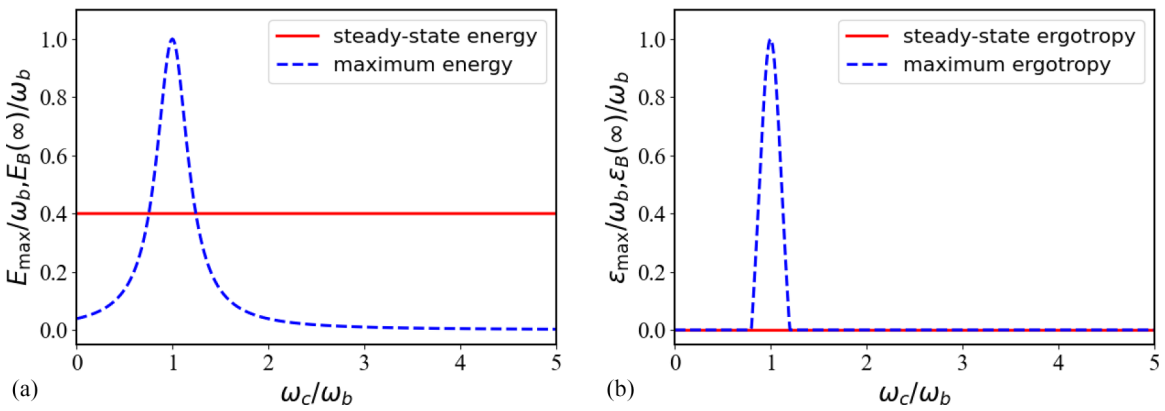

FIG. 12. Panel (a) shows that the maximum energy $E_{\max}$ (dark blue dashed line) in the closed two-qubit system and steady-state energy $E_B(\infty)$ (red solid line) in the thermal bath vary with ω_c/ω_b changes. Panel (b) shows that the maximum ergotropy $\varepsilon_{\max}$ (dark blue dashed line) in the closed two-qubit system and steady-state ergotropy $\varepsilon_B(\infty)$ (red solid line) in the thermal bath vary with ω_c/ω_b changes. Here $\omega_b = 1$, $g = 0.1, \gamma = 1, n_B = 2$.

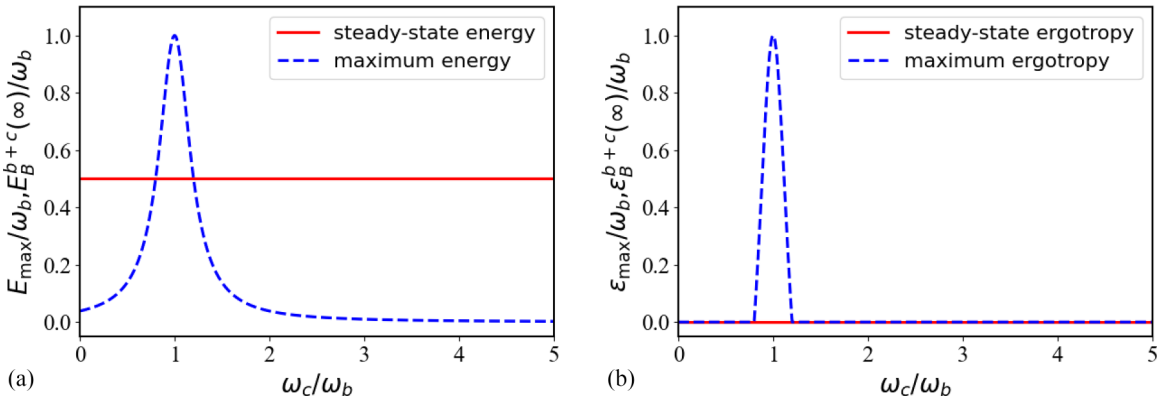

FIG. 13. Panel (a) shows that the maximum energy $E_{\max}$ (dark blue dashed line) in the closed two-harmonic-oscillator system and steady-state energy $E_B^{b+c}(\infty)$ (red solid line) in the phase-flip noisy environment vary with ω_c/ω_b changes. Panel (b) shows that the maximum ergotropy $\varepsilon_{\max}$ (dark blue dashed line) in the closed two-harmonic-oscillator system and steady-state ergotropy $\varepsilon_B^{b+c}(\infty)$ (red solid line) in the phase-flip noisy environment vary with ω_c/ω_b changes. The other parameters are same as Fig. 7.

where ω_c is the frequency of the charger, ω_b is the frequency of the battery, and g is the coupling strength of the battery and charger. Here, b, c ($b^\dagger$, $c^\dagger$) are the boson annihilation (creation) operators for the battery and charger.

Considering that the battery is a qubit, the charger is a harmonic oscillator, the total Hamiltonian can be written as

$$H_3 = \omega_b \frac{\sigma_B^z}{2} + \omega_c c^\dagger c + g(c^\dagger \sigma_B^- + c\sigma_B^+), \tag{A2}$$

where ω_c is the frequency of the charger, ω_b is the energy level spacing of the battery, and g is the coupling strength of the battery and charger. Here, $\sigma_B^{x,y,z}$ represents the Pauli operator acting on the battery, and $\sigma_B^{\pm} = (\sigma_B^x \pm i\sigma_B^y)/2$ represent the up and down operators of the qubit. In addition, c ($c^\dagger$) is the boson annihilation (creation) operator for the charger.

Assume that the battery is in the ground state and the charger is in the excited state at the initial time. For the above two models, we calculate the $E_{\max}$ and $\varepsilon_{\max}$ in the closed system and the $E_B^{b+c}(\infty)$ and $\varepsilon_B^{b+c}(\infty)$ in the phase-flip noisy environment with the change of ω_c/ω_b, as shown in Figs. 13 and 14. Moreover, we also consider the case that the environment is a thermal bath which acts on the charger. For the above two models, we calculate the $E_{\max}$ and $\varepsilon_{\max}$ in the closed system and the $E_B^{b+c}(\infty)$ and $\varepsilon_B^{b+c}(\infty)$ in the thermal bath with the change of ω_c/ω_b, as shown in Figs. 15 and 16. The conclusions are verified in the two-harmonic-oscillator and harmonic-oscillator-qubit models that when ω_b is a constant and $|\omega_c/\omega_b - 1|$ reaches a certain value, the $E_B^{b+c}(\infty)$ and $\varepsilon_B^{b+c}(\infty)$ in the phase-flip noisy environment and the thermal bath will always be greater than or equal to the $E_{\max}$ and $\varepsilon_{\max}$ of the corresponding closed system.

APPENDIX B

Let the initial state of the central-spin model be $|\psi_0\rangle = |0\rangle_b \otimes |m\rangle_c$ ($m = 5$), and consider the case where both the charger and battery are exposed to bit-flip noise. We calculate the maximum energy $E_{\max}$ and ergotropy $\varepsilon_{\max}$ in the closed central-spin system and the steady-state energy $E_B^{b+c}(\infty)$ and ergotropy $\varepsilon_B^{b+c}(\infty)$ in the bit-flip noisy environment with the change of h/B, as shown in Fig. 17. We find that the central-spin model in bit-flip noise is still consistent with the

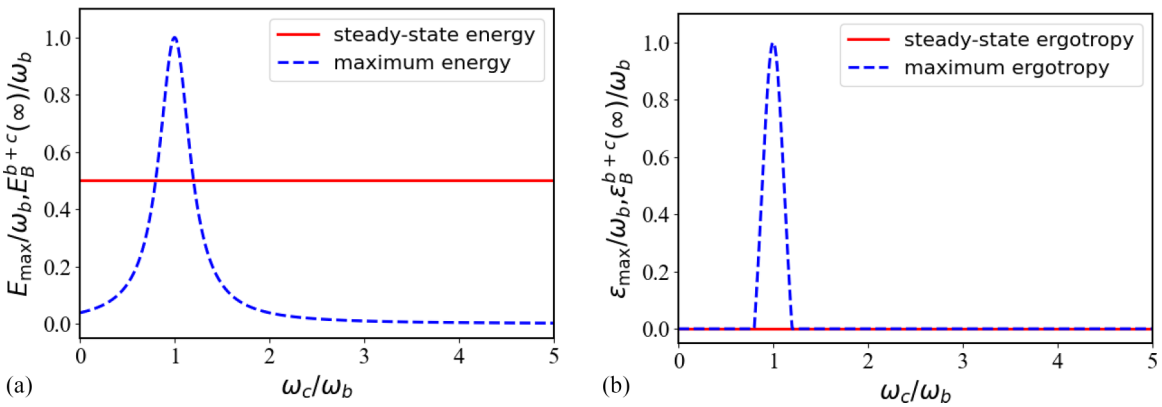

FIG. 14. Panel (a) shows that the maximum energy $E_{\max}$ (dark blue dashed line) in the closed harmonic-oscillator-qubit system and steady-state energy $E_B^{b+c}(\infty)$ (red solid line) in the phase-flip noisy environment vary with ω_c/ω_b changes. Panel (b) shows that the maximum ergotropy $\varepsilon_{\max}$ (dark blue dashed line) in the closed harmonic-oscillator-qubit system and steady-state ergotropy $\varepsilon_B^{b+c}(\infty)$ (red solid line) in the phase-flip noisy environment vary with ω_c/ω_b changes. The other parameters are same as Fig. 7.

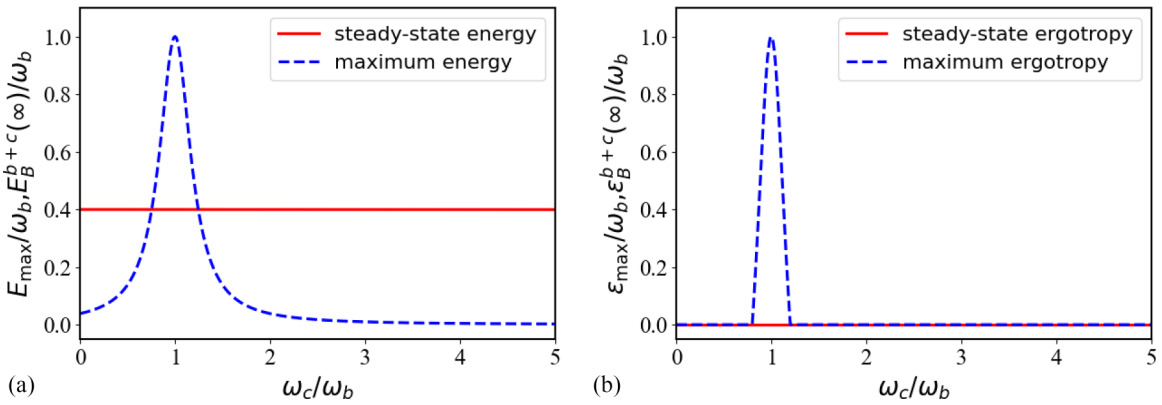

FIG. 15. Panel (a) shows that the maximum energy $E_{\max}$ (dark blue dashed line) in the closed two-harmonic-oscillator system and steady-state energy $E_B^{b+c}(\infty)$ (red solid line) in the thermal bath vary with ω_c/ω_b changes. Panel (b) shows that the maximum ergotropy $\varepsilon_{\max}$ (dark blue dashed line) in the closed two-harmonic-oscillator system and steady-state ergotropy $\varepsilon_B^{b+c}(\infty)$ (red solid line) in the thermal bath vary with ω_c/ω_b changes. The other parameters are same as Fig. 12.

conclusion in Sec. III B. That is, in a central-spin system, when B is a constant and $|h/B-1|$ reaches a certain value, the $E_B^{b+c}(\infty)$ and $\varepsilon_B^{b+c}(\infty)$ in the bit-flip noisy environment will always be greater than or equal to the $E_{\max}$ and $\varepsilon_{\max}$ in the corresponding closed system. We demonstrate this result in the two-qubit model, as shown in Fig. 18. Similarly, we can get this conclusion in the two-harmonic-oscillator and harmonic-oscillator-qubit models.

APPENDIX C

In Figs. 9, 12–16, 18, we note that the $E_{\max}$ and $\varepsilon_{\max}$ of the two-qubit, two-harmonic-oscillator, and harmonic-oscillator-qubit models change the same with ω_b in the closed case. To explain this phenomenon, we give the analytical expressions of $E_{\max}$ and $\varepsilon_{\max}$ of the three models.

When the battery and charger are qubits, the Hamiltonian is Eq. (13). Since the system dynamics of two quibts are enclosed in a two-dimensional subspace consisting of $|g_b, e_c\rangle$ and $|e_b, g_c\rangle$, the Hamiltonian of Eq. (13) can be rewritten as a matrix:

$$H_1 = \begin{bmatrix} (\omega_c-\omega_b)/2 & g \\ g & (\omega_b-\omega_c)/2 \end{bmatrix}, \tag{C1}$$

where $|g_b\rangle$ and $|e_b\rangle$ ($|g_c\rangle$ and $|e_c\rangle$) represent the ground state and excited state of the battery (charger), respectively. The eigenvalues of the Hamiltonian are $E_+ = \sqrt{g^2+[(\omega_c-\omega_b)/2]^2}$ and $E_- = -\sqrt{g^2+[(\omega_c-\omega_b)/2]^2}$. The corresponding eigenstates are $|\psi_+\rangle = (X|g_b, e_c\rangle + |e_b, g_c\rangle)/\alpha$ and $|\psi_-\rangle = (Y|g_b, e_c\rangle + |e_b, g_c\rangle)/\beta$, where α and β are the normalization constants of $|\psi_+\rangle$ and $|\psi_-\rangle$, $X = (\omega_c-\omega_b)/2g + \sqrt{g^2+[(\omega_c-\omega_b)/2]^2}/g$, $Y = (\omega_c-\omega_b)/2g - \sqrt{g^2+[(\omega_c-\omega_b)/2]^2}/g$. The initial moment of the battery is in the ground state, the charger is in the excited state, and the evolution equation of the initial state over time can be expressed as

$$\begin{aligned} |\psi(t)\rangle &= e^{-iH_1 t}|g_b, e_c\rangle = e^{-iH_1 t}\frac{(\alpha|\psi_+\rangle - \beta|\psi_-\rangle)}{X-Y} \\ &= \frac{\alpha e^{-iE_+ t}|\psi_+\rangle - \beta e^{-iE_- t}|\psi_-\rangle}{X-Y}. \end{aligned} \tag{C2}$$

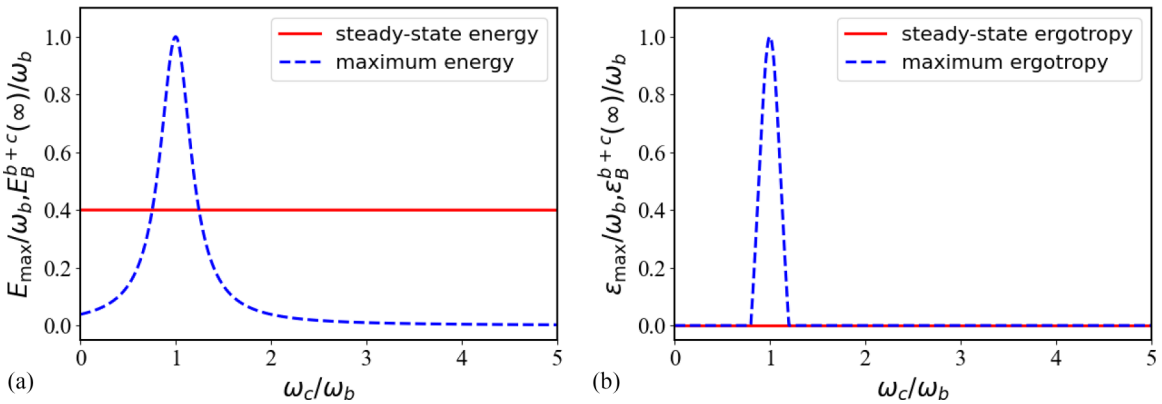

FIG. 16. Panel (a) shows that the maximum energy $E_{\max}$ (dark blue dashed line) in the closed harmonic-oscillator-qubit system and steady-state energy $E_B^{b+c}(\infty)$ (red solid line) in the thermal bath vary with ω_c/ω_b changes. Panel (b) shows that the maximum ergotropy $\varepsilon_{\max}$ (dark blue dashed line) in the closed harmonic-oscillator-qubit system and steady-state ergotropy $\varepsilon_B^{b+c}(\infty)$ (red solid line) in the thermal bath vary with ω_c/ω_b changes. The other parameters are same as Fig. 12.

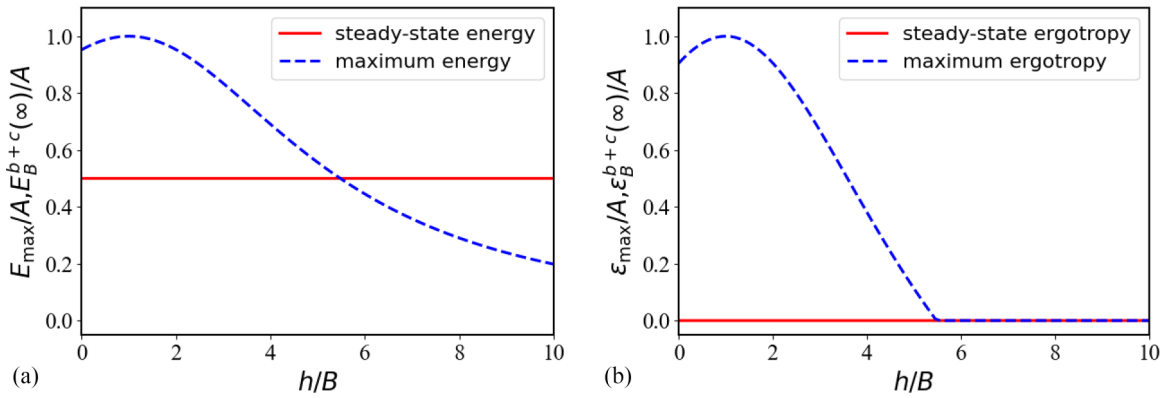

FIG. 17. Panel (a) shows the variations of maximum energy E_{max} (dark blue dashed line) in the closed central-spin system and steady-state energy $E_B^{b+c}(\infty)$ (red solid line) in the bit-flip noisy environment with h/B. Panel (b) shows the variations of maximum ergotropy ε_{max} (dark blue dashed line) in the closed central-spin system and steady-state ergotropy $\varepsilon_B^{b+c}(\infty)$ (red solid line) in the bit-flip noisy environment with h/B. The other parameters are same as Fig. 6.

At time t, the density matrix of the battery can be written as

$$\rho_B(t) = \mathrm{Tr}_C[|\psi(t)\rangle\langle\psi(t)|] = \langle e_c|\psi(t)\rangle\langle\psi(t)|e_c\rangle + \langle g_c|\psi(t)\rangle\langle\psi(t)|g_c\rangle. \quad \text{(C3)}$$

The free Hamiltonian of the battery is $H_1^B = \omega_b\sigma_B^z/2 = \omega_b(|e_b\rangle\langle e_b| - |g_b\rangle\langle g_b|)/2$. According to Eq. (6)

$$E_B(t) = \mathrm{Tr}\big[H_1^B\rho_B(t)\big] = \frac{\omega_b}{2(X-Y)^2}\{2 - 2\cos(2E_+t) - [X^2 + Y^2 - 2XY\cos(2E_+t)]\}. \quad \text{(C4)}$$

The maximum energy that can be stored in the evolution of a battery is called the maximum energy, that is, $E_{max} = \max[E_B(t) - E_B(0)]$. At the initial moment, the battery is in the ground state, and the ground-state energy is $E_B(0) = -\omega_b/2$. Through calculation, we find that $XY = -1$. So when $\cos(2E_+t) = -1$, $E_B(t)$ has the maximum value. The expression for E_{max} is as follows:

$$E_{max} = \max[E_B(t) - E_B(0)] = \frac{4\omega_b}{(X-Y)^2}. \quad \text{(C5)}$$

We arrange the eigenvalues of the battery Hamiltonian H_1^B in ascending order to obtain $\varepsilon_1 = -\omega_b/2$ and $\varepsilon_2 = \omega_b/2$. The density matrix of the battery over time is written in the matrix form as

$$\rho_B(t) = \begin{bmatrix} \frac{2-2\cos(2E_+t)}{(X-Y)^2} & 0 \\ 0 & \frac{X^2+Y^2-2XY\cos(2E_+t)}{(X-Y)^2} \end{bmatrix}. \quad \text{(C6)}$$

When $X^2 + Y^2 - 2XY\cos(2E_+t) \geqslant 2 - 2\cos(2E_+t)$, that is, $\cos(2E_+t) \leqslant (X^2 + Y^2 - 2)/(2XY - 2)$, we arrange the eigenvalues of the density matrix of the battery in descending order to obtain $r_1 = [X^2 + Y^2 - 2XY\cos(2E_+t)]/(X-Y)^2$ and $r_2 = [2 - 2\cos(2E_+t)]/(X-Y)^2$. According to Eq. (8), $\varepsilon_B(t) = E_B(t) - (r_1\varepsilon_1 + r_2\varepsilon_2)$. According to the calculation, in this case, the ergotropy is 0. So $\varepsilon_{max} = \max[\varepsilon_B(t)] = 0$. When $X^2 + Y^2 - 2XY\cos(2E_+t) \leqslant 2 - 2\cos(2E_+t)$, that is, $\cos(2E_+t) \geqslant (X^2 + Y^2 - 2)/(2XY - 2)$, we arrange the eigenvalues of the density matrix of the battery in descending order to obtain $r_1 = [2 - 2\cos(2E_+t)]/(X-Y)^2$ and $r_2 = [X^2 + Y^2 - 2XY\cos(2E_+t)]/(X-Y)^2$. According to

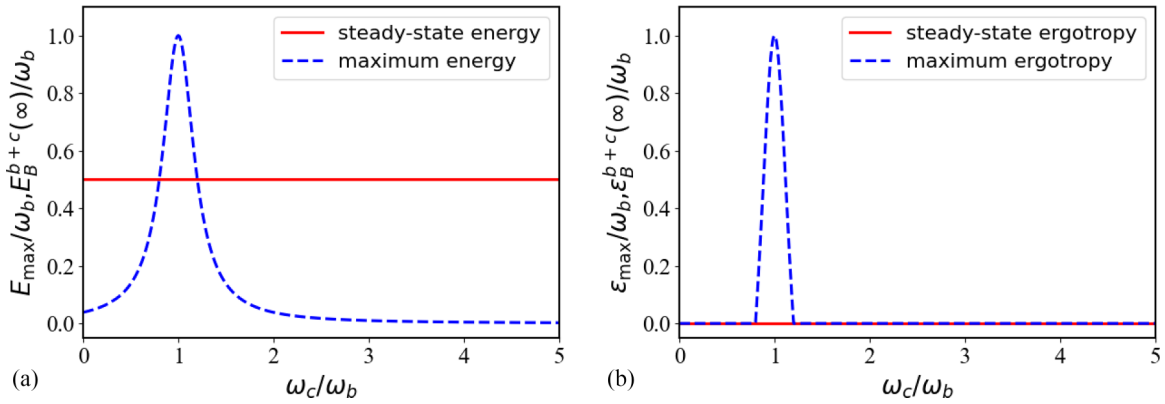

FIG. 18. Panel (a) shows that the maximum energy E_{max} (dark blue dashed line) in the closed two-qubit system and steady-state energy $E_B^{b+c}(\infty)$ (red solid line) in the bit-flip noisy environment vary with ω_c/ω_b changes. Panel (b) shows that the maximum ergotropy ε_{max} (dark blue dashed line) in the closed two-qubit system and steady-state ergotropy $\varepsilon_B^{b+c}(\infty)$ (red solid line) in the bit-flip noisy environment vary with ω_c/ω_b changes. The other parameters are same as Fig. 7.

Eq. (8),

$$\varepsilon_B(t) = E_B(t) - (r_1\varepsilon_1 + r_2\varepsilon_2) = \frac{\omega_b}{(X-Y)^2}[2 - 2\cos(2E_+t) - (X^2 + Y^2 - 2XY\cos(2E_+t)]. \tag{C7}$$

Since $XY = -1$, the ergotropy of the battery can be maximized when $\cos(2E_+t)$ is taken as the minimum value. Bringing the values of X and Y into $(X^2 + Y^2 - 2)/(2XY - 2)$, we can find that $(X^2 + Y^2 - 2)/(2XY - 2) = -(\omega_c - \omega_b)^2/4g^2$. The value range of $(X^2 + Y^2 - 2)/(2XY - 2)$ is $[0, -\infty)$. Since $\cos(2E_+t) \geqslant (X^2 + Y^2 - 2)/(2XY - 2)$, $\varepsilon_{\max}$ needs to be discussed in two cases. In the first case, when $(X^2 + Y^2 - 2)/(2XY - 2) \leqslant -1$, $\cos(2E_+t)$ can obtain a minimum value of -1, and the ergotropy has a maximum value, which is expressed as

$$\varepsilon_{\max} = \frac{\omega_b}{(X-Y)^2}[4 - (X+Y)^2]. \tag{C8}$$

In the second case, when $-1 < (X^2 + Y^2 - 2)/(2XY - 2) \leqslant 0$, $\cos(2E_+t)$ can obtain a minimum value of $(X^2 + Y^2 - 2)/(2XY - 2)$, and the ergotropy has a maximum value. By calculation, we find that the maximum value of the ergotropy is equal to 0.

Using the same approach, we can analytically calculate the $E_{\max}$ and $\varepsilon_{\max}$ of two-harmonic-oscillator and harmonic-oscillator-qubit models. We find that the $E_{\max}$ and $\varepsilon_{\max}$ of these models are same as the two-qubit model. Considering that the harmonic oscillator and qubit are two-dimensional, by comparing the Hamiltonian of the harmonic oscillator and the qubit, we can find that they choose different ground states, but the energy level spacing is the same. In the study of quantum battery, we focus on the change in energy and ergotropy, which is related to the spacing of energy levels. So, we can see that the dark blue dashed lines in Figs. 9, 12–16, 18 are the same.

[1] R. Alicki and M. Fannes, Entanglement boost for extractable work from ensembles of quantum batteries, Phys. Rev. E **87**, 042123 (2013).

[2] K. V. Hovhannisyan, M. Perarnau-Llobet, M. Huber, and A. Acín, Entanglement generation is not necessary for optimal work extraction, Phys. Rev. Lett. **111**, 240401 (2013).

[3] F. Campaioli, F. A. Pollock, F. C. Binder, L. Céleri, J. Goold, S. Vinjanampathy, and K. Modi, Enhancing the charging power of quantum batteries, Phys. Rev. Lett. **118**, 150601 (2017).

[4] L. P. García-Pintos, A. Hamma, and A. del Campo, Fluctuations in extractable work bound the charging power of quantum batteries, Phys. Rev. Lett. **125**, 040601 (2020).

[5] D. Ferraro, M. Campisi, G. M. Andolina, V. Pellegrini, and M. Polini, High-power collective charging of a solid-state quantum battery, Phys. Rev. Lett. **120**, 117702 (2018).

[6] D. Rossini, G. M. Andolina, and M. Polini, Many-body localized quantum batteries, Phys. Rev. B **100**, 115142 (2019).

[7] D. Rosa, D. Rossini, G. M. Andolina, M. Polini, and M. Carrega, Ultra-stable charging of fast-scrambling SYK quantum batteries, J. High Energ. Phys. 11 (2020) 067.

[8] L. Peng, W. B. He, S. Chesi, H. Q. Lin, and X. W. Guan, Lower and upper bounds of quantum battery power in multiple central spin systems, Phys. Rev. A **103**, 052220 (2021).

[9] X. Y. Yang, Y. H. Yang, M. Alimuddin, R. Salvia, S. M. Fei, L. M. Zhao, S. Nimmrichter, and M. X. Luo, Battery capacity of energy-storing quantum systems, Phys. Rev. Lett. **131**, 030402 (2023).

[10] A. Delmonte, A. Crescente, M. Carrega, D. Ferraro, and S. Sassetti, Characterization of a two-photon quantum battery: Initial conditions, stability and work extraction, Entropy **23**, 612 (2021).

[11] J. X. Liu, H. L. Shi, Y. H. Shi, X. H. Wang, and W. L. Yang, Entanglement and work extraction in the central-spin quantum battery, Phys. Rev. B **104**, 245418 (2021).

[12] S. Julià-Farré, T. Salamon, A. Riera, M. N. Bera, and M. Lewenstein, Bounds on the capacity and power of quantum batteries, Phys. Rev. Res. **2**, 023113 (2020).

[13] F. H. Kamin, F. T. Tabesh, S. Salimi, and A. C. Santos, Entanglement, coherence, and charging process of quantum batteries, Phys. Rev. E **102**, 052109 (2020).

[14] H. L. Shi, S. Ding, Q. K. Wan, X. H. Wang, and W. L. Yang, Entanglement, coherence, and extractable work in quantum batteries, Phys. Rev. Lett. **129**, 130602 (2022).

[15] L. Wang, S. Q. Liu, F. L. Wu, H. Fan, and S. Y. Liu, Two-mode Raman quantum battery dependent on coupling strength, Phys. Rev. A **108**, 062402 (2023).

[16] J. Q. Quach, K. E. McGhee, L. Ganzer, D. M. Rouse, B. W. Lovett, E. M. Gauger, J. Keeling, G. Cerullo, D. G. Lidzey, and T. Virgili, Superabsorption in an organic microcavity: Toward a quantum battery, Sci. Adv. **8**, eabk3160 (2022).

[17] F. Q. Dou and F. M. Yang, Superconducting transmon qubit-resonator quantum battery, Phys. Rev. A **107**, 023725 (2023).

[18] S. Ghosh, T. Chanda, S. Mal, and A. Sen(De), Fast charging of a quantum battery assisted by noise, Phys. Rev. A **104**, 032207 (2021).

[19] V. Shaghaghi, V. Singh, M. Carrega, D. Rosa, and G. Benenti, Lossy micromaser battery: almost pure states in the jaynescummings regime, Entropy **25**, 430 (2023).

[20] S. Gherardini, F. Campaioli, F. Caruso, and F. C. Binder, Stabilizing open quantum batteries by sequential measurements, Phys. Rev. Res. **2**, 013095 (2020).

[21] A. C. Santos, Quantum advantage of two-level batteries in the self-discharging process, Phys. Rev. E **103**, 042118 (2021).

[22] S. Y. Bai and J. H. An, Floquet engineering to reactivate a dissipative quantum battery, Phys. Rev. A **102**, 060201(R) (2020).

[23] D. Farina, G. M. Andolina, A. Mari, M. Polini, and V. Giovannetti, Charger-mediated energy transfer for quantum batteries: An open-system approach, Phys. Rev. B **99**, 035421 (2019).

[24] J. Q. Quach and W. J. Munro, Using dark states to charge and stabilize open quantum batteries, Phys. Rev. Appl. **14**, 024092 (2020).

[25] M. Carrega, A. Crescente, D. Ferraro, and M. Sassetti, Dissipative dynamics of an open quantum battery, New J. Phys. **22**, 083085 (2020).

[26] F. Barra, Dissipative charging of a quantum battery, Phys. Rev. Lett. **122**, 210601 (2019).

[27] F. Zhao, F. Q. Dou, and Q. Zhao, Quantum battery of interacting spins with environmental noise, Phys. Rev. A **103**, 033715 (2021).

[28] K. Xu, H. J. Zhu, G. F. Zhang, and W. M. Liu, Enhancing the performance of an open quantum battery via environment engineering, Phys. Rev. E **104**, 064143 (2021).

[29] K. Xu, H. G. Li, Z. G. Li, H. J. Zhu, G. F. Zhang, and W. M. Liu, Charging performance of quantum batteries in a double-layer environment, Phys. Rev. A **106**, 012425 (2022).

[30] F. H. Kamin, F. T. Tabesh, S. Salimi, F. Kheirandish, and A. C. Santos, Non-Markovian effects on charging and self-discharging process of quantum batteries, New J. Phys. **22**, 083007 (2020).

[31] M. T. Mitchison, J. Goold, and J. Prior, Charging a quantum battery with linear feedback control, Quantum **5**, 500 (2021).

[32] Y. Yao and X. Q. Shao, Optimal charging of open spin-chain quantum batteries via homodyne-based feedback control, Phys. Rev. E **106**, 014138 (2022).

[33] Y. Yao and X. Q. Shao, Stable charging of a Rydberg quantum battery in an open system, Phys. Rev. E **104**, 044116 (2021).

[34] S. Tirone, R. Salvia, S. Chessa, and V. Giovannetti, Work extraction processes from noisy quantum batteries: The role of nonlocal resources, Phys. Rev. Lett. **131**, 060402 (2023).

[35] M. B. Arjmandi, H. Mohammadi, and A. C. Santos, Enhancing self-discharging process with disordered quantum batteries, Phys. Rev. E **105**, 054115 (2022).

[36] A. G. Catalano, S. M. Giampaolo, O. Morsch, V. Giovannetti, and F. Franchini, Frustrating quantum batteries, arXiv:2307.02529.

[37] A. Faribault, H. Koussir, and M. H. Mohamed, Read-Green points and level crossings in XXZ central spin models and $p_x + ip_y$ topological superconductors, Phys. Rev. B **100**, 205420 (2019).

[38] W. Yao, R. B. Liu, and L. J. Sham, Theory of electron spin decoherence by interacting nuclear spins in a quantum dot, Phys. Rev. B **74**, 195301 (2006).

[39] Ł. Cywiński, W. M. Witzel, and S. Das Sarma, Electron spin dephasing due to hyperfine interactions with a nuclear spin bath, Phys. Rev. Lett. **102**, 057601 (2009).

[40] A. Faribault and D. Schuricht, Integrability-based analysis of the hyperfine-interaction-induced decoherence in quantum dots, Phys. Rev. Lett. **110**, 040405 (2013).

[41] M. W. Doherty, N. B. Manson, P. Delaney, F. Jelezko, J. Wrachtrup, and L. C. L. Hollenberg, The nitrogen-vacancy colour centre in diamond, Phys. Rep. **528**, 1 (2013).

[42] M. A. Nielsen and I. L. Chuang, *Quantum Computation and Quantum Information: 10th Anniversary Edition* (Cambridge University Press, Cambridge, England, 2010).

[43] F. Mayo and A. J. Roncaglia, Collective effects and quantum coherence in dissipative charging of quantum batteries, Phys. Rev. A **105**, 062203 (2022).

[44] F. T. Tabesh, F. H. Kamin, and S. Salimi, Environment-mediated charging process of quantum batteries, Phys. Rev. A **102**, 052223 (2020).

[45] F. Tacchino, T. F. F. Santos, D. Gerace, M. Campisi, and M. F. Santos, Charging a quantum battery via nonequilibrium heat current, Phys. Rev. E **102**, 062133 (2020).

[46] G. D. Chiara, G. Landi, A. Hewgill, B. Reid, A. Ferraro, A. J. Roncaglia, and M. Antezza, Reconciliation of quantum local master equations with thermodynamics, New J. Phys. **20**, 113024 (2018).

[47] W. L. Yu, Y. Zhang, H. Li, G. F. Wei, L. P. Han, F. Tian, and J. Zou, Enhancement of charging performance of quantum battery via quantum coherence of bath, Chin. Phys. B **32**, 010302 (2023).